ARENA Project RND009 - Report on key failure modes of PV modules in the field

This report provides a detailed description of key module failure modes in the field, their causes, and their detection with PL monitoring techniques developed in this ARENA-funded project.

The rapid expansion of the photovoltaic (PV) industry combined with a steep drop in manufacturing costs and module prices has caused the reliability of PV modules to become a primary focus. Standard qualification of module reliability by accelerated stress testing is mandatory, for example as described in the IEC 61215standard for qualification of crystalline silicon (c-Si) modules [1]. However this can only verify performance in the initial phase following installation, and cannot be used to guarantee long-term reliability within the full warranty period [2, 3]. In many cases degradation modes that lead to module failure will only become evident following field exposure, and can result in financial losses from reduced power output, or in the worst case, safety concerns. A robust method for detection of degradation and failure modes of modules, and ideally a way to predict the performance of modules and future failure modes, is therefore a requirement for both manufacturers and system owners.

Crystalline silicon (c-Si) solar technology currently captures > 90% of the market for PV modules [4]. For that reason, almost all available degradation and failure mode data reported here is obtained from c-Si modules. Recent work by Jordan *et al.* [5] provided an extensive review of c-Si module failure modes from observations on installations commissioned over the last 35 years. They identified a number of key failure modes based on occurrence rate and severity and observed that the prevalence of specific faults is strongly dependent on the age of the installation and its climate. A summary of the findings from [5] is shown in the appendix, which details the percentage of modules surveyed that exhibited each failure mode. A synopsis of each failure mode, its causes, and its identification using the prototype module imaging tool developed at UNSW Sydney over the course of this project [6] are provided below. This tool is capable of acquiring line scan photoluminescence (PL_{LS}) images of commercial modules with up to 72 full area cells.

Encapsulant discolouration

Also called yellowing or browning (due to its appearance ranging from light yellow to dark brown), encapsulant discolouration is the most common failure mode reported, particularly in older installations. It is typically caused by photodegradation of the EVA material used for encapsulation by ultraviolet (UV) light, which decreases light transmittance to the active regions of the module resulting in reduced light-generated current [7]. Although the impact of this on performance is often fairly minor, encapsulant discolouration highly impacts module appearance and hence qualifies as a failure.

Encapsulant discolouration can be identified by visual inspection once it has reached a certain level of severity, but at this level it will already have a negative impact on power output. It is hence beneficial to detect the onset of the defect earlier. This can be achieved using PL_{LS} imaging, since encapsulant discolouration luminesces strongly with a broad spectrum [8]. A demonstration of this is shown on a cell from a field degraded module in Figure 1: the visual image shows no indication of encapsulant discolouration, whilst a large central rectangular region of increased luminescence intensity as a result of encapsulant discolouration is visible in the PL_{LS} image. Visual and PL_{LS} images of a cell from a different field degraded module with severe encapsulant discolouration are shown in Figure 2 for comparison.

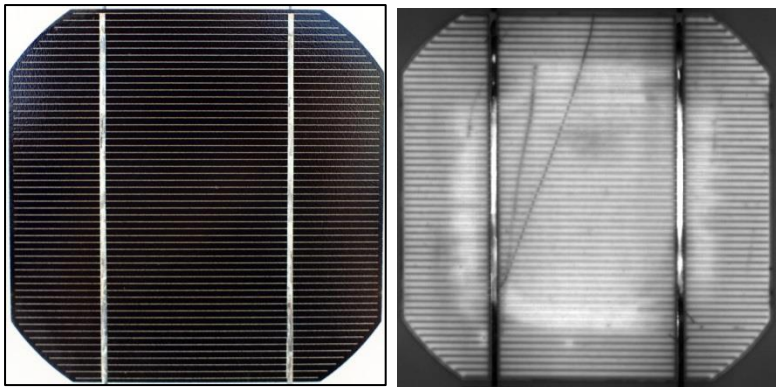

(a) (b)

Figure 1: Images of a cell from a field degraded module exhibiting the onset of encapsulant discolouration. (a) Visual image. (b) PL_{LS} image.

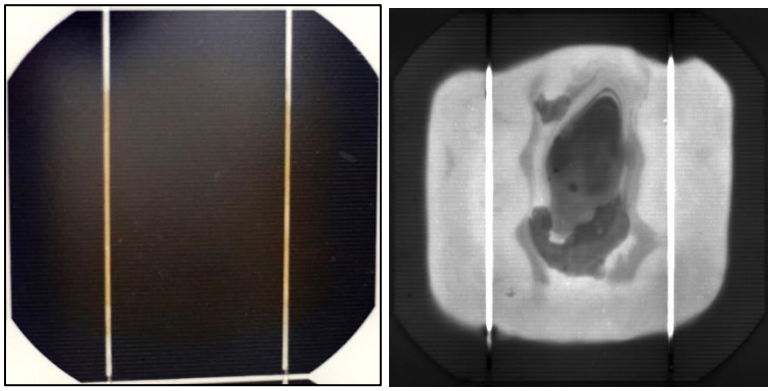

(a) (b)

Figure 2: Images of a cell from a field degraded module exhibiting severe encapsulant discolouration. (a) Visual image. (b) PL_{LS} image.

Series resistance increase

Encapsulation of a module by lamination is necessary to provide a barrier to protect it from environmental factors. If the encapsulation of the module is compromised for any reason, ingress of moisture can occur and may corrode the internal metal circuitry. Although this results in a darkening (discolouration) of the metallisation that can be identified with a visual inspection as demonstrated in Figure 3a, it is usually accompanied by an increase in series resistance (R_S) at the affected area. High R_S inhibits the extraction of current from a module, which hence reduces its power output, ultimately resulting in a failure.

Identification of R_S defects is possible in a PL_{LS} image, because the narrow line illumination used for photoexcitation only illuminates a small portion of the module at any time. This forms a voltage difference between the illuminated and non-illuminated regions, causing lateral current to flow that changes magnitude with variations in R_S [6, 9, 10]. Regions of high R_S appear with increased luminescence intensity compared to the rest of the sample and are easy to identify, an example of which is shown in Figure 3b in the centre of the cell. Our group has previously demonstrated that it is also possible to quantify the severity of a R_S increase from a PL_{LS} image, as the luminescence contrast around the defect correlates strongly with its impact on power loss [11, 12].

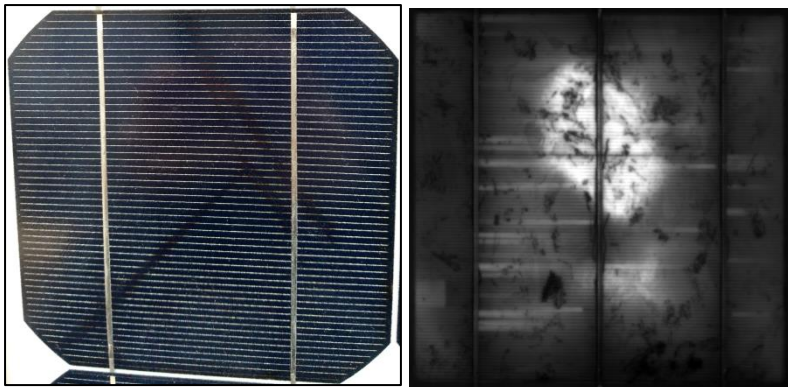

(a) (b)

Figure 3: (a) Visual image of a cell with internal circuitry discolouration. (b) PL_{LS} image of a cell with a large oval region of increased series resistance (R_S).

Fractured cells

Also called cell cracks, fractured cells are very difficult to avoid and their impact on module power output is often hard to predict. For example micro cracks (smaller than 30 µm in width [13]) have a negligible impact on power output, but act as a starting point for the propagation of larger cell cracks during handling/transport and mechanical loading during field operation from wind, thermal cycling and snow [14, 15]. Severe cracks can electrically isolate regions of a cell in a module, resulting in a current loss proportional to the size of the affected region and a reduction in power output. When the affected region exceeds approximately 5% of the total cell area, the associated loss in short circuit current has a severe impact on the total power output of the corresponding sub-string in the module and results in failure.

Cell cracks appear as irregular lines with very low luminescence intensity in PL_{LS} images, as observed in Figure 4a. Fully and partially electrically isolated regions caused by cell cracks have an increased luminescence intensity compared to the rest of the cell in PL_{LS} images, since current is unable (or less likely) to be electrically extracted from the affected region, and generates excess luminescence. Two examples of electrically isolated regions are shown in Figure 4b at the top of the cell.

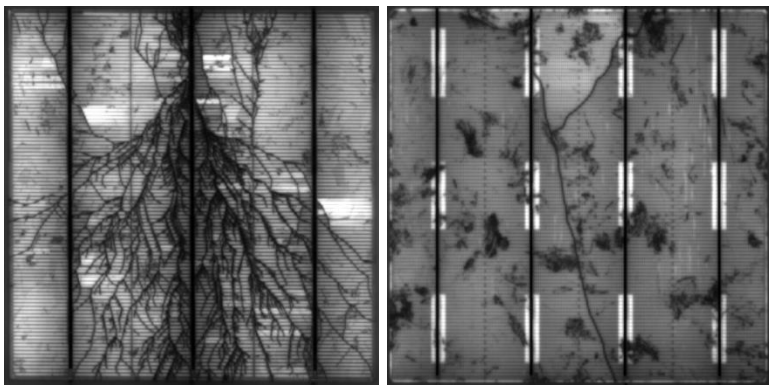

(a) (b)

Figure 4: PL_{LS} images of (a) cell with extensive cell cracking and (b) cell with two electrically isolated regions at the top of the cell.

Diode/junction box

The module junction box is an enclosure that contains the electrical connections of each sub-string, and the bypass diodes used to prevent damage to the cells from reverse bias if the module is partially shaded.

A number of different failures can occur within the junction box, but the most common ones are failures of the bypass diodes. These include shunted bypass diodes, disconnected (open circuit) bypass diodes or bypass diodes installed with incorrect polarity. A defective bypass diode will fail to prevent high voltage reverse biasing of the shaded cell, which can cause irreversible hot spot damage as a result of highly localised heating with temperatures higher than 150 °C. This can lead to encapsulant deterioration, delamination, and in the worst case fire [16].

Detection of bypass diode failures is more complicated, since they have no role in the normal operation of a module. The simplest method is to measure the reverse dark current-voltage (IV) characteristics of the module, which is an additional feature of our prototype module imaging tool. It is more difficult to identify these defects using PL_{LS} imaging. An example of reverse dark IV analysis on a module with a bypass diode failure is shown in Figure 5. The experimentally measured data agrees best with simulated data of a module with one shunted and two operational bypass diodes, indicating that this is the cause of the failure.

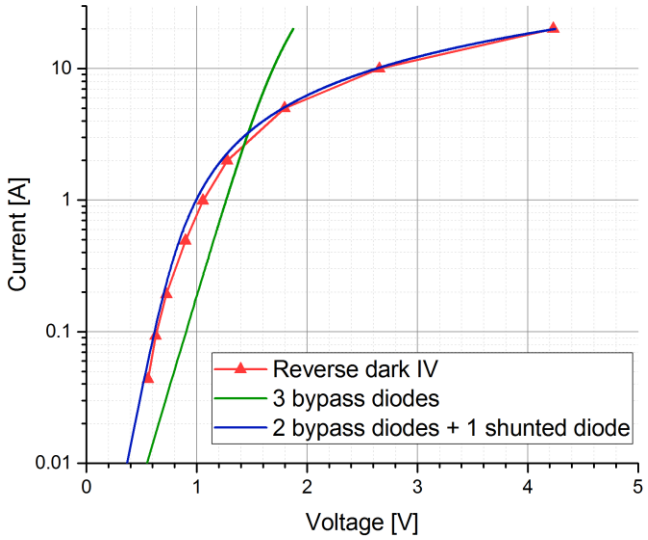

Figure 5: Reverse dark IV measurement (red symbols) of a module, compared with simulated reverse dark IV characteristics of a module with three operational bypass diodes (green line), and a module with one shunted and two operational bypass diodes (blue line).

The results from the above simple dark IV analysis are consistent with EL imaging data of the module, which show that an entire string of the module is dark (Fig.6a). What happens in this case is that the shunted bypass diode carries the entire dark forward current, bypassing the cells in that string, which is why they do not emit any EL signal. The PL image, on the other hand, is unaffected by the shunted bypass diode. While in this case the EL image information alone allows unambiguous assessment of the defect type, the situation is less clear for other scenarios, such as open circuit diodes, for which EL images would not provide any information.

Summary

Different types of defects appear with different image features in EL_{LS} and in PL_{LS} images, respectively. The most robust defect detection is therefore enabled by a combination of these two imaging modes.

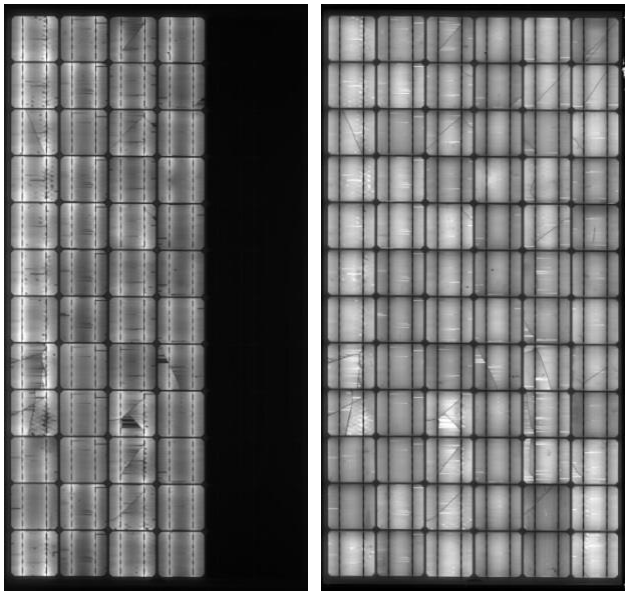

(a) (b)

Figure 6: (a) EL_{LS} image and (b) PL_{LS} image of an industrial c-Si module with a shunted bypass diode. The bypass diode routes the forward dark current past the cells in the righthand side string in the EL image.

Appendix: Summary Table [5]

	Climate	Moderate					Hot and humid				Desert			
	Date of installation	pre-2000			post-2000		pre-2000		post-2000		pre-2000		post-2000	
	Field exposure (years)	0-10	11-20	20+	0-10	11-20	11-20	20+	0-10	11-20	0-10	11-20	0-10	11-20
Degradation mode	No. modules surveyed	2311	8683	976	457	1626	360	188	2718	170	188	4890	1451	4103
Encapsulant discolouration		99.2%	67.1%	50.5%	0%	0%	87.4%	100%	9.9%	100%	100%	95.1%	3.3%	23.2%
Internal circuitry discolouration/ series resistance increase		1.9%	0%	28.7%	4.0%	0.6%	28.0%	79.7%	9.9%	1.5%	0%	0.5%	2.8%	19.5%
Fractured cells		47.5%	1.2%	6.5%	0.5%	0.1%	3.1%	63.0%	5.0%	10.6%	0%	1.0%	1.7%	1.9%
Diode/junction box		1.9%	0%	1.2%	0%	0%	58.9%	18.0%	21.7%	0%	0%	0%	0.1%	0.7%

References

[1] International Electrotechnical Commission, IEC 61215-1:2016, Terrestrial photovoltaic (PV) modules - Design qualification and type approval - Part 1: Test requirements

[2] C. R. Osterwald and T. J. McMahon, "History of accelerated and qualification testing of terrestrial photovoltaic modules: A literature review," *Progress in Photovoltaics: Research and Applications*, vol. 17, pp. 11-33, January 2009.

[3] A. Masuda, C. Yamamoto, N. Uchiyama, K. Ueno, T. Yamazaki, K. Mitsuhashi, A. Tsutsumida, J. Watanabe, J. Shirataki, and K. Matsuda, "Sequential and combined acceleration tests for crystalline Si photovoltaic modules," *Japanese Journal of Applied Physics*, vol. 55, pp. 1-7, 2016.

[4] VDMA Photovoltaic Equipment, "International Technology Roadmap for Photovoltaic (ITRPV) 2016 Results including maturity report, Eighth Edition," September 2017.

[5] D. C. Jordan, T. J. Silverman, J. H. Wohlgemuth, S. R. Kurtz, and K. T. VanSant, "Photovoltaic failure and degradation modes," *Progress in Photovoltaics: Research and Applications*, vol. 25, pp. 318-326, April 2017.

[6] I. Zafirovska, M. K. Juhl, J. W. Weber, O. Kunz, and T. Trupke, "Module Inspection Using Line Scanning Photoluminescence Imaging," in *32nd European Photovoltaic Solar Energy Conference and Exhibition (32nd EU PVSEC)*, Munich, Germany, 2016, pp. 1826-1829.

[7] A. W. Czanderna and F. J. Pern, "Encapsulation of PV modules using ethylene vinyl acetate copolymer as a pottant: A critical review," *Solar Energy Materials & Solar Cells*, vol. 43, pp. 101-181, September 1996.

[8] F. J. Pern, I. L. Eisgruber, and R. H. Micheels, "Spectroscopic, scanning laser OBIC and I-V/QE characterizations of browned EVA solar cells," in *IEEE 25th Photovoltaic Specialists Conference (PVSC)*, Washington, DC, USA 1996, pp. 1255-1258.

[9] M. Kasemann, L. M. Reindl, and B. Michl, "Contactless Qualitative Series Resistance Imaging on Solar Cells," *IEEE Journal of Photovoltaics*, vol. 2, pp. 181-183, April 2012.

[10] J.-M. Wagner, J. Carstensen, A. Berhane, A. Schütt, and H. Föll, "Serial resistance analysis with the shaded luminescence technique," in *26th European Photovoltaic Solar Energy Conference and Exhibition (26th EU PVSEC)*, Hamburg, Germany, 2011, pp. 1569-1575.

[11] I. Zafirovska, M. K. Juhl, J. W. Weber, J. Wong, and T. Trupke, "Detection of Finger Interruptions in Silicon Solar Cells Using Line Scan Photoluminescence Imaging," *IEEE Journal of Photovoltaics*, vol. 7, pp. 1496-1502, November 2017.

[12] I. Zafirovska, M. K. Juhl, and T. Trupke, "Efficient Detection of Finger Interruptions from Photoluminescence Images," in *33rd European Photovoltaic Solar Energy Conference and Exhibition (33rd EU PVSEC)*, Amsterdam, The Netherlands, 2017, pp. 1689-1693.

[13] Y.-C. Chiou, J.-Z. Liu, and Y.-T. Liang, "Micro crack detection of multi-crystalline silicon solar wafer using machine vision techniques," *Sensor Review*, vol. 31, pp. 154-165, 2011.

[14] M. Köntges, S. Kajari-Schröder, I. Kunze, and U. Jahn, "Crack Statistic of Crystalline Silicon Photovoltaic Modules," in *26th European Photovoltaic Solar Energy Conference and Exhibition (26th EU PVSEC)*, Hamburg, Germany, 2011, pp. 3290-3294.

[15] S. Kajari-Schröder, I. Kunze, and M. Köntges, "Criticality of Cracks in PV Modules," *Energy Procedia*, vol. 27, pp. 658-663, 2012.

[16] W. Herrmann, W. Wiesner, and W. Vaassen, "Hot spot investigations on PV modules-new concepts for a test standard and consequences for module design with respect to bypass diodes," in *IEEE 26th Photovoltaic Specialists Conference (PVSC)*, Anaheim, CA, USA, 1997, pp. 1129-1132.